Materials Science and Engineering A 552 (2012) 76–80

Contents lists available at SciVerse ScienceDirect

Materials Science and Engineering A

journal homepage: www.elsevier.com/locate/msea

Effects of cold rolling and solid solution treatments on mechanical properties of β-phase Mg–14.3Li–0.8Zn alloy

S.K. Wu [a], J.Y. Wang [b,*], K.C. Lin [a], H.Y. Bor [c]

[a] Department of Materials Science and Engineering, National Taiwan University, Taipei 106, Taiwan
[b] Department of Materials Science and Engineering, National Dong-Hwa University, Hwa-Lian 974, Taiwan
[c] Metallurgy Section, Materials and Optoelectronics Research Division, Chung Shan Institute of Science and Technology, Taoyuan 325, Taiwan

ARTICLE INFO

Article history:
Received 10 August 2011
Received in revised form 29 March 2012
Accepted 30 April 2012
Available online 15 May 2012

Keywords:
Magnesium alloy
Mechanical properties
Cold-rolling
Solid-solution treatment
Strengthening effect

ABSTRACT

Cold rolled and solid-soluted (SS) treatments are employed to improve mechanical properties of ultra-light Mg–14.3Li–0.8Zn (LZ141) alloy. As-homogenized LZ141 alloy is mainly β-phase with few α-phase particles and exhibits quite good workability. Its tensile strength, elongation and hardness are 122 MPa, 40% and 41.6 Hv, respectively. For the specimen SS at 400 °C × 40 min and a subsequent 80% cold-rolling, the alloy's tensile strength, elongation and hardness are 227 MPa, 33% and 61.0 Hv, respectively. XRD tests reveal that, for the severely cold-rolled specimen, the preferred orientation changes, while for the SS specimen, it remains unchanged. The duplex strengthening effect of solid-solution with subsequently severe cold-rolling can significantly improve mechanical properties of LZ141 alloy.

1. Introduction

The importance of light metals has been widely recognized in the efforts to reduce environmental contamination and energy consumption. Among all structural metals, magnesium is the lightest with its density as low as 1.74 g/cm^3. Magnesium alloys, highly valued in transportation and 3C electronic industries, exhibit outstanding properties in heat dissipation, vibration resistance and electromagnetic shielding [1,2]. These advantages, however, have been offset by the hexagonal close-packed (HCP) structure of magnesium, a property which leads to difficulty in processing and forming at room temperature. To compensate for this drawback, lithium has been added to change the alloys crystal structure and thus improve the formability of Mg alloys. Meanwhile, the added lithium in Mg alloys can facilitate the light weight design by further reducing the alloys' density. The Mg–Li binary phase diagram indicates that, when the amount of the lithium added in Mg exceeds ≈11 wt% (the alloys' compositions used in this study are always in wt%), the crystal structure of Mg–Li alloys changes from α (HCP) structure of Mg solid solution to β (BCC) structure of Li solid solution [3]. The β-phase Mg–Li alloys not only reduce their density to below 1.5 g/cm^3, but also improve their formability at room temperature [4,5]. However, binary β-phase Mg–Li alloys are seldom used in engineering field due to their relatively low strength, low thermal and creep resistance, and thus ternary/quaternary β-phase alloys are designed to overcome these disadvantages. In 1955, Jones studied the strength and work-hardening properties of ternary magnesium β-alloys containing lithium with a Mg: Li ratio of 88: 12. He pointed out that alloys with Cd, Zn or Al produce optimum properties in the cast and rolled condition but are not stable at ordinary temperature. On the other hand, alloys with Si, Cu, Sn or Ce (or misch metal) have poor mechanical properties [5]. In 1957, Clark and Sturkey investigated the age-hardening of Mg–19.6Li–18.5Zn β-alloy and found that it age-hardens rapidly at room temperature and reaches the hardness peak after 20–30 h aging by the formation of $MgLi_2Zn$ precipitates, a transition structure of the equilibrium LiZn phase [6]. In 1980, Alamo and Barchik studied the precipitation phenomena of Mg–11.4Li–1.4Al β-alloy and confirmed that, for specimens solid-soluted and then aged at room temperature, phase reaction follows $\beta \rightarrow \beta + \theta + \alpha$ and the hardness reaches its maximum value when θ phase precipitates. Here the θ is a metastable phase of the equilibrium LiAl one [7]. In 1997, Saito et al. investigated the aging behavior and mechanical properties of Mg–16.0Li–0.7Al–0.5Cu β-alloy and found that, for specimens solid-soluted at 450 °C for 1 h and then quenched in iced-water, the maximum tensile strength of 198 MPa with an elongation of 15% can be obtained when the solid-soluted specimen was aged at room temperature for ≈1400 h to the hardness peak [8]. In 2002, Takuda et al. studied the tensile property of Mg–12Li–1Zn β-alloy thin sheets that were annealed at 350 °C for 0.5 h and then hot-rolled at the same temperature to a thickness of 0.6 mm. They observed that the β grains are elongated with

* Corresponding author. Tel.: +886 3 8634230; fax: +886 3 8634200.
E-mail address: jy-wang@yahoo.com.tw (J.Y. Wang).

0921-5093/$ – see front matter © 2012 Elsevier B.V. All rights reserved.
http://dx.doi.org/10.1016/j.msea.2012.04.118

textural change and have sufficiently high ductility at low strain rates. The tensile strength of the specimen in the rolling direction tested at room temperature is 125 MPa with an elongation of 56% [9]. In 2006, Chang et al. studied the mechanical properties of Mg–11Li–1Zn β-alloy containing small amount of α-phase processed by equal channel angular extrusion and got an ultimate tensile strength of 175 MPa with an elongation of 35% [10]. In 2008, Hsu et al. investigated the room temperature aging characteristic of Mg–11.2Li–0.95Al–0.43Zn β-alloy which was extruded at 210 °C with an extrusion ratio of 29.4:1, solid-soluted at 400 °C for 0.5 h and then quenched in water. Its tensile strength and elongation tested at room temperature along the extruding direction are 123 MPa and 96%, respectively [11].

As mentioned above, aluminum and zinc are the most common elements added to Mg–Li β-alloys to improve the strength and work-hardening properties, but they impair the ductility. The Mg–Li–Zn and Mg–Li–Al ternary β-alloys can be strengthened by cold-/hot- working. The reported study indicated that Mg–Li–Zn β-alloys containing up to 5% Zn could be cold-rolled readily and Mg–Li–Al β-alloys containing 1–4% Al could be hot-rolled [5]. Solid-solution treatment is another effective method to strengthen ternary Mg–Li β-alloys. Previous literature indicated that, for solid-soluted and quenched Mg–Li and Mg–Zn alloys, Zn is approximately three times more effective than Al in increasing the yield strength for alloys [12,13]. However, the ultimate tensile strength of ternary Mg–Li β-alloys strengthened by cold-/hot- working or solid-solution treatment seldom exceeded 200 MPa due to the intrinsic low strength of binary Mg–Li β-alloys. At the same time, the strengthened ternary Mg–Li β-alloys are not stable even if aged at room temperature because of the precipitation of metastable phase such as $MgLi_2Zn$ precipitates in Mg–19.6Li–18.5Zn alloy [6] and θ precipitates in Mg–11.4Li–1.4Al alloy [7]. In this study, duplex strengthening method, i.e., solid-solution treatment first and followed by severe cold-rolling at room temperature is used to improve the strength and the stability of Mg–Li β-alloys. The samples used in this study were cold rolled to reach 80% in thickness reduction and thus the Mg–Li β-alloys should have superior cold-rolling workability. Therefore, Mg–14Li–1Zn (ASTM LZ141) β-alloy is selected to study, as pointed out in Ref [5] that Mg–Li–Zn β-alloys containing up to 5% Zn could be cold-rolling readily. The effects of both cold rolling and solid-solution treatments on the mechanical properties of ultra-light LZ141 alloy are investigated. In addition, the duplex strengthening effect of solid-solution and severe subsequent cold-rolling treatment on the mechanical properties of LZ141 alloy is also studied. The improvement in tensile strength of thermo-mechanically treated LZ141 alloy compared with that of as-homogenized alloy is also discussed.

2. Experimental procedures

High purity Mg and Zn raw materials were melted by vacuum induction melting under argon atmosphere. Pure lithium element was added into the molten alloy to obtain the composition of LZ141 alloy and then the molten liquid was cast into a steel mold (size: 390 mm × 80 mm × 310 mm) for solidification. The cast ingot was homogenized at 350 °C for 12 h and cut into plates with a thickness of 10–20 mm. The chemical composition of the homogenized plate, Mg–14.3Li–0.8Zn alloy, was measured using ICP-OES and the result is listed in Table 1.

Table 1
The composition of as-homogenized LZ141 specimen (in wt%) measured by ICP-OES.

Mg	Li	Al	Zn	Mn	Fe
Balance	14.26	0.018	0.827	0.012	0.007

The density of as-homogenized LZ141 alloy, 1.379 g/cm^3, measured by using Archimede's principle, was substantially lower than that of commercial AZ80 alloy (1.802 g/cm^3) [14] and the densities of some engineering polymers.

Cold rolling was conducted at room temperature by using a BDR 150 × 200 2HI-MILL rolling machine manufactured by Daito Seiki Co., Japan. The thickness reduction for each rolling pass was limited to no more than 0.7 mm to avoid cracking. For solid-solution treatment, the specimens were heated at 400 °C for 40 min and then water-quenched. For microstructural examination, the specimens were prepared by the standard metallographic procedure with an etching solution of 1 ml 2, 4, 6-Trinitrophenol, 1 ml water, and 7 ml ethanol. Microstructures observations were performed using a Nikon optical microscope (OM) and a Philips XL-30 scanning electron microscope (SEM). ASTM E112-88 standard was used to calculate the average grain size. The crystal structures were detected by using PANalytical X'Pert PRO XRD with Cu K_α under a scanning rate of 4°/min. Microvickers hardness, Hv, was measured by a Mitutoyo HM hardness tester with the applied load and time of 100 g and 15 s, respectively. The reported Hv data were the average of at least 10 measurements for each specimen. Tensile tests were carried out by a Shimadzu AG-IS 50 KN testing machine with a strain rate of 1 mm/min. The dimension of tensile specimens is 35 mm × 5 mm × 1 mm with a gauge length of 10 mm.

3. Results and discussion

3.1. As-homogenized LZ141 alloy

The OM image of as-homogenized LZ141 alloy in Fig. 1(a) shows an equiaxial microstructure with uniform grain size distribution and an average grain size of 264 μm. The SEM image of Fig. 1(a), shown in Fig. 1(b), reveals some white, spherical-like particles within the grains and along the grain boundaries. Fig. 2 shows the XRD pattern of as-homogenized LZ141 alloy. As seen from Fig. 2(a), LZ141 alloy is mainly β-phase with little α-phase. This characteristic can be confirmed indisputably from Fig. 2(b), which is the enlarged profile of Fig. 2(a) in the 2θ range of 30–45°. The XRD result of Fig. 2 indicates that the white particles shown in Fig. 1(b) are α-phase. According to the Mg–Li binary phase diagram [3], only a single β phase exists in the Mg–14Li binary alloy. However, Fig. 1(b) and Fig. 2 show that a trace of α phase still remains in LZ141 alloy. This result implies that it is difficult to remove α-phase completely in ternary Mg–Li–X alloys. A similar phenomenon was also observed in the study of LA141 alloy, but no explanation was made as to the cause for the appearance of α-phase [15].

The hardness of as-homogenized LZ141 alloy is found to be 41.6 Hv. This value is a little lower than the average hardness of Mg–16Li–2Zn alloy (LZ162), 50 Hv [16]. The intrinsic low hardness is due to its high Li-content and coarse grain size, as well as the lack of the aluminum strengthening effect. Crawford et al. [17] mentioned that, even though LA141 alloy has the solid-soluted Al atoms for strengthening, its strength improvement is insignificant but its elongation is much sacrificed.

3.2. Cold-rolled LZ141 alloy

Fig. 3(a) and (b) show the OM images of cold-rolled LZ141 alloy after 54% and 80% cold-rolling, respectively. As shown in Fig. 3(a), many curved gliding bands developed in some grains, but some other grains remained unchanged, just as they were before cold-rolling. The hardness of 54% cold-rolled alloy is 54.9 Hv, which is much higher than that of as-homogenized one. When the specimen's cold-rolling is increased to 80%, as shown in Fig. 3(b), a large amount of curved gliding bands appear and the original grain shape

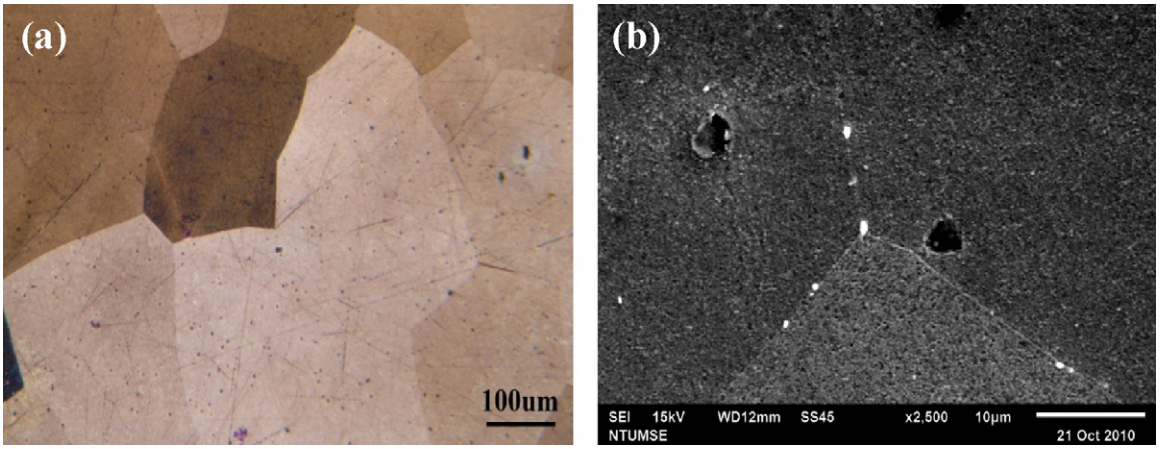

Fig. 1. (a) Optical micrograph, (b) SEM image of as-homogenized LZ141 specimen. The white spherical-like particles are observed along grain boundaries and in the grains.

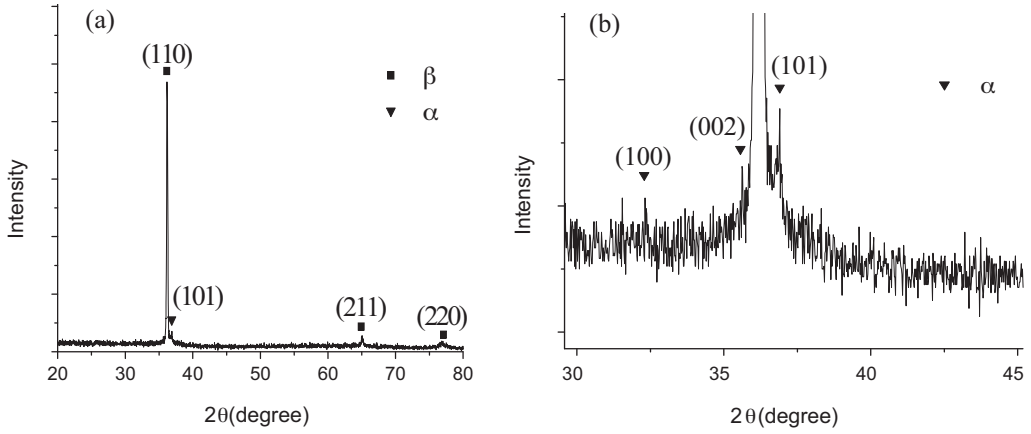

Fig. 2. (a) The XRD pattern of as-homogenized LZ141 specimen, (b) the enlarged profile from the local portion of (a) in the 2θ range of 30–45°.

is no longer discernable. The hardness of 80% cold-rolled specimen, 58.9 Hv is slightly higher than that of the sample cold-rolled at 54%. The hardness of both 54% and 80% cold-rolled specimens has no significant change even when they are aged at room temperature for 216 h. This phenomenon may be due to the lack of precipitated phase in LZ141 alloy. The XRD pattern of 80% cold-rolled LZ141 alloy is shown in Fig. 4. According to this result, β-phase with a trace of α-phase is mainly present in severely cold-rolled LZ141 alloy,

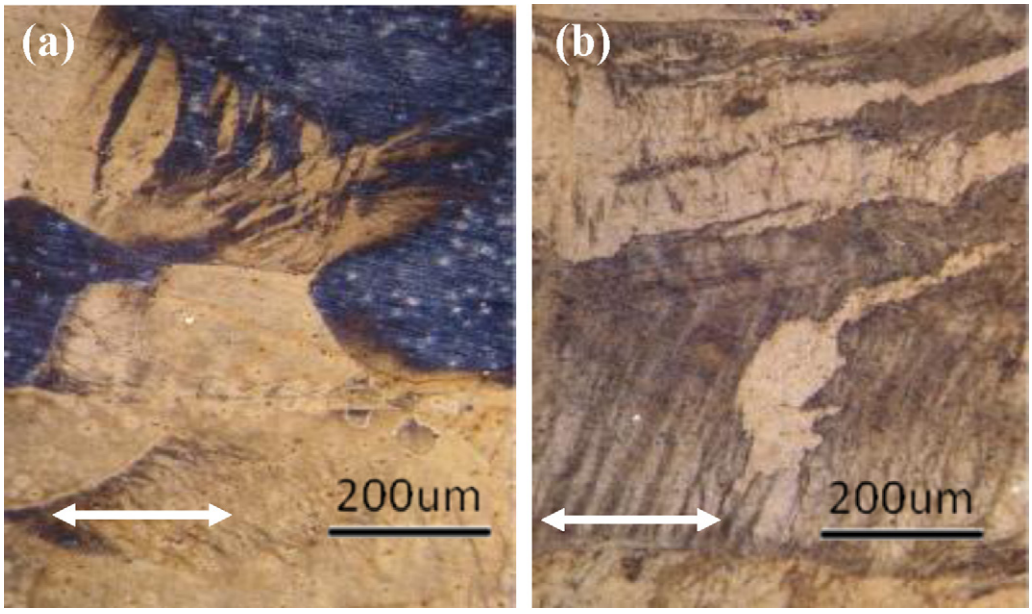

Fig. 3. Optical micrographs of the specimens cold-rolled at room temperature by (a) 54%, (b) 80% thickness reduction. The arrow indicates the rolling direction.

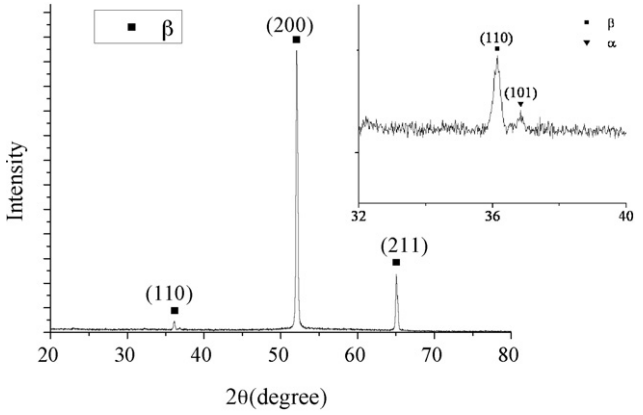

Fig. 4. The XRD pattern of LZ141 specimen after 80% cold-rolling at room temperature.

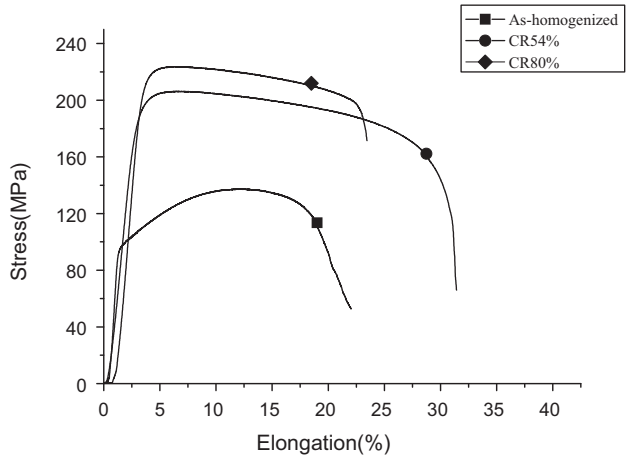

Fig. 5. The tensile stress-strain curves of as-homogenized, 54% and 80% cold rolled LZ141 specimens.

as shown in the insert of Fig. 4. Comparing the peaks in Fig. 2(a) and Fig. 4, one can see that the peak with the strongest intensity occurred at $(1\,1\,0)_\beta$ for as-homogenized specimen, but changed to $(2\,0\,0)_\beta$ for 80% cold-rolled specimen. This feature suggests that the preferred orientation of LZ141 plate can be induced by the cold-rolling process, but more study is required for verification. Fig. 5 shows the tensile stress-strain curves of as-homogenized, 54% and 80% cold-rolled LZ141 specimens. From Fig. 5, the tensile strength and elongation of as-homogenized LZ141 alloy are 122 MPa and 40%, respectively. After 54% cold-rolling, owing to the cold-working

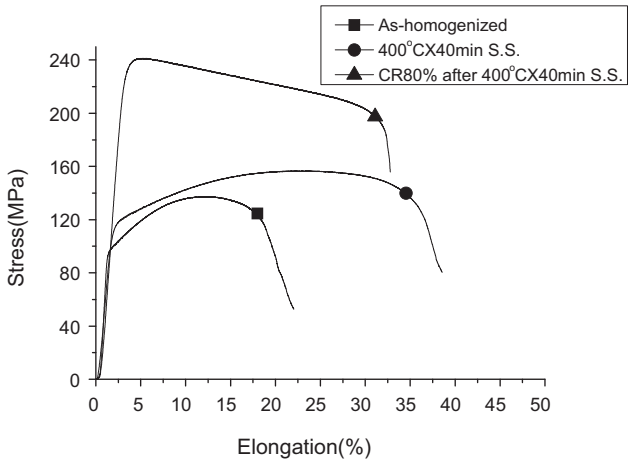

Fig. 7. The stress-strain curves of LZ141 specimens solid-soluted at 400 °C × 40 min (SS) and SS with subsequent 80% cold-rolling. The stress-strain curve of as-homogenized specimen is also plotted for comparison.

effect, the tensile strength increased to 177 MPa and the elongation decreased to 31%. For 80% cold-rolled specimen, the tensile strength increased to 202 MPa but the elongation decreased to 23%. The decrease of the elongation was possibly caused by the dislocations pile-ups due to excessive cold-rolling.

3.3. Solid-soluted LZ141alloy

Fig. 6(a) and (b) show the OM images of the specimens solid-soluted (SS) at 400 °C × 40 min and SS with subsequent 80% cold-rolling, respectively. As seen from Fig. 6(a), no noticeable change in the grain size (259 μm) was observed in SS specimen, as compared with the as-homogenized alloy. The hardness of SS specimen is 46.0 Hv. Fig. 6(b) shows the presence of massive gliding bands in the grains, and the hardness increased to 61.0 Hv due to the duplex strengthening effects caused by solid-soluted hardening and work hardening. Fig. 7 shows the tensile stress-strain curves of LZ141 specimens after SS and SS with subsequent 80% cold-rolling. From Fig. 7, the tensile strength and elongation of SS specimen increased to 146 MPa and 38%, respectively. Fig. 8 shows the XRD pattern of SS LZ141 specimen in which only the peaks of β-phase can be observed. This feature indicates that, in SS specimen, the α-phase particles are soluted into the β-phase matrix. The substantial increase in tensile strength of SS specimen comes from the fact that the α-phase particles are solid-soluted in the β-phase. This characteristic also reduces the resistance of grain boundary gliding and dislocation movement, thus giving rise to the good elongation observed in the SS specimen. Fig. 7 also shows

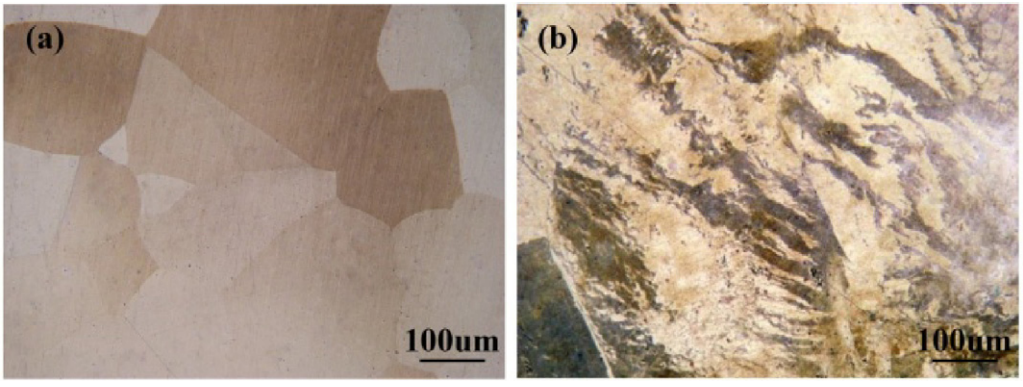

Fig. 6. Optical micrographs of LZ141 specimens (a) solid-soluted at 400 °C × 40 min, (b) as (a) and a subsequent 80% cold-rolling.

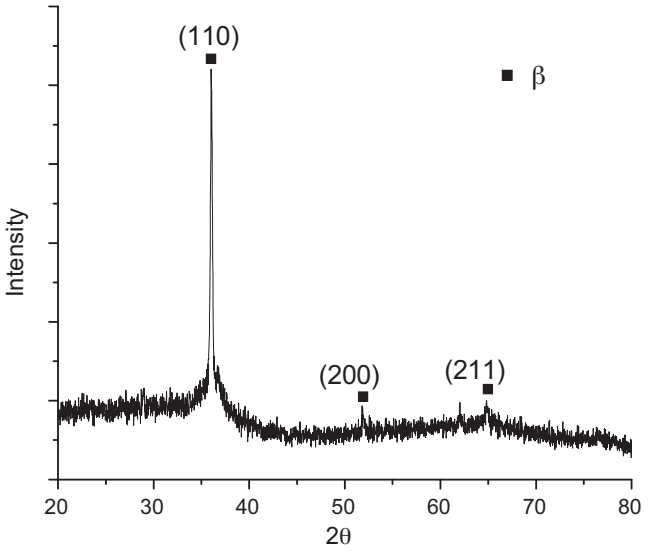

Fig. 8. The XRD pattern of LZ141 specimen solid-soluted at 400 °C × 40 min.

that the specimen SS with subsequent 80% cold-rolling can further increase the tensile strength to 227 MPa while retaining the elongation at approximately 33%. Obviously, the mechanical properties of LZ141 alloy can be significantly improved by the duplex strengthening effects mentioned earlier. Fig. 8 also demonstrates that, for SS specimen, the peak with the strongest intensity is $(0\,1\,1)_\beta$, not $(2\,0\,0)_\beta$, a result which is similar to that of as-homogenized one. This phenomenon indicated that the solid-solution treatment did not change the alloy's preferred orientation.

4. Conclusions

Several alloys of Mg–14.3Li–0.8Zn (LZ141)- as-homogenized, cold-rolled, SS and severely cold-rolled- were studied for microstructural observations, hardness/tensile tests and XRD measurements. Experimental results show that as-homogenized LZ141 alloy is mainly β-phase with trace amount of tiny α-phase particles present along grain boundaries and in the grains. The average grain size, density, tensile strength, elongation and hardness are 264 μm, 1.379 g/cm^3, 122 MPa, 40% and 41.6 Hv, respectively. As-homogenized LZ141 alloy exhibits good workability and can be cold-rolled to 80% thickness reduction in which massive gliding bands develop in the grains. For specimen cold-rolled to 80% thickness reduction, the tensile strength, elongation and hardness are 202 MPa, 23% and 58.9 Hv, respectively. The XRD pattern indicates that the preferred orientation changed from $(1\,1\,0)_\beta$ for as-homogenized specimen to $(2\,0\,0)_\beta$ for specimens that were severely cold-rolled, but the preferred orientation remained unchanged for specimen SS at 400 °C × 40 min. The SS LZ141 alloy, compared with as-homogenized sample, showed a tensile strength of 146 MPa and elongation of 38% due to solid-soluted of the α-phase particles in the β-matrix. The grain size of SS specimen is 259 μm, about the same as that of as-homogenized one. If SS specimen is further cold-rolled to 80% thickness reduction, the tensile strength, elongation and hardness can reach 227 MPa, 33% and 61.0 Hv, respectively. Experimental results showed that duplex strengthening effects caused by solid-solution with subsequently severe cold-rolling can significantly improve the mechanical properties of LZ141 alloy.

Acknowledgement

The authors gratefully acknowledge the financial support of this study from National Science Council (NSC), Taiwan, Republic of China, under the grants NSC98-2623-E002-014-D, NSC99-2221-E-259-003- and NSC100-2623-E002-010-D.

References

[1] ASM International. Handbook Committee (Ed.), Metals Handbook, Vol. 2, Nonferrous Alloys and Special-Purpose Materials, 10th ed., ASM International, Ohio, USA, 1990, p. 480.
[2] Y. Kojima, S. Kamado, Mater. Sci. Forum 488–489 (2005) 9–16.
[3] H. Bake (Ed.), ASM Handbook, Vol. 3, Alloy Phase Diagrams, ASM International, Ohio, USA, 1992, pp. 2–276.
[4] O. Sivakesavam, Y.V.R.K. Prasad, Mater. Sci. Eng. A 323 (2002) 270–277.
[5] W.R.D. Jones, J. Inst. Met. 84 (1955–1956) 364–378.
[6] J.B. Clark, L. Sturkey, J. Inst. Met. 86 (1957–1958) 272–276.
[7] A. Alamo, A.D. Banchik, J. Mater. Sci. 15 (1980) 222–229.
[8] N. Saito, M. Mabuchi, M. Nakanishi, K. Kubota, K. Higashi, Scr. Mater. 36 (1997) 551–555.
[9] H. Takuda, H. Matsusaka, S. Kikuchi, K. Kubota, J. Mater. Sci. 37 (2002) 51–57.
[10] T.C. Chang, J.Y. Wang, C.L. Chu, S. Lee, Mater. Lett. 60 (2006) 3272–3276.
[11] C.C. Hsu, J.Y. Wang, S. Lee, Mater. Trans. 49 (2008) 2728–2731.
[12] I.J. Polymear, Light Alloys, 4th ed., Elsevier B/H, London, 2006, pp. 284–285.
[13] T.B. Abbott, M.A. Easton, C.H. Cáceres, in: G.E. Totten, L. Xie, K. Funatani (Eds.), Handbook of Mechanical Alloy Design, Marcel Dekker Inc, New York, 2004, p. 501.
[14] S.H. Chang, S.K. Wu, W.L. Tsai, J.Y. Wang, J. Alloys Compd. 487 (2009) 142–145.
[15] T. Liu, S.D. Wu, S.X. Li, P.J. Li, Mater. Sci. Eng. A 460–461 (2007) 499–503.
[16] H.B. Ji, G.C. Yao, H.B. Li, J. Univ. Sci. Technol. Beijing 15 (2008) 440–443.
[17] P. Crawford, R. Barrosa, J. Mendez, J. Foyos, O.S. Es-Said, J. Mater. Process. Technol. 56 (1996) 108–118.